Production of top quark pairs in association with a hard gluon to order α_s^2

A. Brandenburg[a,b]

Institut für Theoretische Physik, RWTH Aachen, D-52056 Aachen, Germany

Abstract. The production of top quark pairs accompanied by a hard gluon in e^+e^- annihilation is studied including next-to-leading order corrections in the strong coupling. At leading order, the fraction r of $t\bar{t}g$ events with respect to all $t\bar{t}$ events is computed analytically as a function of the minimal gluon energy. Next-to-leading order results for r are given for center-of-mass energies of 0.5 and 1 TeV. We further calculate the differential distribution of r with respect to several variables, including the top quark energy and the $t\bar{t}$ invariant mass. We then investigate how our results depend on the choice of the renormalization scheme for the top quark mass by comparing results expressed in terms of either the pole mass or the $\overline{\text{MS}}$ mass. Finally we estimate the sensitivity of the fraction r on the value of the running top quark mass at a scale of 1 TeV.

1 Introduction

A future high-energy e^+e^- collider will open up a new domain for the experimental investigation of the fundamental interactions between elementary particles. In particular, the production of top quark pairs in a clean environment will offer many interesting opportunities both to perform precision tests of Quantum Chromodynamics (QCD) and to probe possible deviations from the standard theory. For example, the total cross section for $e^+e^- \to t\bar{t}$ has been computed recently to next-to-next-to-leading order in the strong coupling α_s both in the threshold region [1–3] and also far above threshold [4]. The results obtained for the threshold region will allow for a very precise determination of the top quark mass [5–7].

The subject of this paper is the production of top quark pairs above threshold accompanied by (at least) one additional parton with a hard momentum. To be more explicit, we are interested in the reaction

$$e^+(p_+) + e^-(p_-) \to t(k_t) + \bar{t}(k_{\bar{t}}) + X(k_X), \qquad (1)$$

and we require that the parton(s) X carry a large momentum k_X. At order α_s, the additional parton can only be a gluon, and at order α_s^2 we have the possibilities $X = g, gg, q\bar{q}$. By determining the properties of a final state with three or more partons one can test the strong interactions in great detail as is well known from the extensive studies of jets in e^+e^- annihilation. For example, by comparing the cross section for (1) (which will be precisely

defined in the next section) to the inclusive $t\bar{t}$ production cross section, one could measure α_s. Any deviation from the standard determination of α_s using event samples containing light quark jets would indicate a violation of the "flavour independence" of the strong interactions — i.e., would point towards new physics phenomena. A specific example of non-standard interactions that could be probed by reaction (1) are possible anomalous couplings of the top quark to photons, Z-bosons and gluons. In [8] it has been shown that a large anomalous chromomagnetic $t\bar{t}g$ coupling would modify the gluon energy spectrum in $e^+e^- \to t\bar{t}g$. Furthermore, symmetry tests can be performed utilizing the richer kinematic structure of the final state in (1). These contain tests of the CP symmetry [9] and the search for final state rescattering effects using triple momentum correlations [10]. Both the search for heavy quark anomalous couplings [11] and the symmetry tests [12] have been shown to be experimentally feasible in the case of $b\bar{b}g$ production at the Z resonance, and it will be interesting to see whether similar studies are possible with top quarks.

For any of the above studies it is mandatory to analyse reaction (1) at next-to-leading order in α_s, which is the topic of this paper. It is organized as follows: We start in Sect. 2 by studying reaction (1) at leading order. We derive an analytic formula for the fraction r of $t\bar{t}g$ events with respect to all $t\bar{t}$ events as a function of the minimal gluon energy. In Sect. 3 we discuss the QCD corrections to reaction (1). We evaluate the fraction r at next-to-leading order for center-of-mass energies of 0.5 and 1 TeV. We further compute the differential distribution of the cross section for reaction (1), normalized to the total $t\bar{t}$ cross section, with respect to the top quark energy, the $t\bar{t}$ in-

variant mass, and the cosine of the angle between the t and $\bar{t}$. In Sect. 4 we study the dependence of our results on both the renormalization scale and the renormalization scheme employed to define the top quark mass. We first review the dependence of the total $t\bar{t}$ cross section on the mass renormalization scheme by expressing the result to order α_s in terms of either the perturbative pole mass or the $\overline{\text{MS}}$ (running) mass. We then study in the same fashion the scheme and scale dependence of the fraction r. Finally we estimate, for a c.m. energy of 1 TeV, the sensitivity of the fraction r on the value of the running top quark mass.

2 Analysis at leading order

In this section we discuss in some detail reaction (1) at leading order (LO) in α_s, i.e., the production of a $t\bar{t}$ pair together with a single gluon,

$$e^+(p_+) + e^-(p_-) \to t(k_t) + \bar{t}(k_{\bar{t}}) + g(k_g). \tag{2}$$

We start by defining the following dimensionless variables:

$$x = \frac{2kk_t}{s} = \frac{2E_t}{\sqrt{s}},$$

$$\bar{x} = \frac{2kk_{\bar{t}}}{s} = \frac{2E_{\bar{t}}}{\sqrt{s}},$$

$$x_g = \frac{2kk_g}{s} = \frac{2E_g}{\sqrt{s}} = 2 - x - \bar{x},$$

$$x_{t\bar{t}} = \frac{(k_t + k_{\bar{t}})^2}{s} = 1 - x_g, \tag{3}$$

where $\sqrt{s}$ is the center-of-mass energy, $k = p_+ + p_-$, and $E_{t,\bar{t},g}$ are the energies of the final state particles in the c.m. system. The cross section for reaction (2) develops a soft singularity as $E_g \to 0$. An infrared finite cross section may be defined by demanding

$$x_g > x_{\text{cut}}, \tag{4}$$

where x_{cut} is some preset number. This condition avoids the region of phase space where the gluon becomes soft. Due to the finite mass of the top quark no collinear (mass) singularities arise and thus the above condition is sufficient to define an infrared finite cross section. The requirement (4) does *not* lead to a finite cross section for $e^+e^- \to q\bar{q}g$, where q is a massless quark, because the latter cross section is also singular when the gluon is collinear to the (anti-)quark.

We want to study the fraction r of $t\bar{t}g$ events for which $x_g > x_{\text{cut}}$ with respect to all $t\bar{t}$ events. Since x_g is no useful variable for final states with four or more partons (which will be relevant at higher orders in α_s), we use instead the scaled $t\bar{t}$ invariant mass square $x_{t\bar{t}}$ defined in (3), i.e. replace the condition $x_g > x_{\text{cut}}$ by the (at LO equivalent) condition:

$$1 - x_{t\bar{t}} > x_{\text{cut}}. \tag{5}$$

The fraction r is defined as

$$r(x_{\text{cut}}) = \frac{\sigma\left(e^+e^- \to t\bar{t}X;\ 1 - x_{t\bar{t}} > x_{\text{cut}}\right)}{\sigma_{\text{tot}}(e^+e^- \to t\bar{t})}$$

$$\equiv \frac{\sigma_3(x_{\text{cut}})}{\sigma_{\text{tot}}}. \tag{6}$$

At LO we have $X = g$ and write:

$$r(x_{\text{cut}}) = \frac{\alpha_s}{2\pi} \frac{\sigma_3^0(x_{\text{cut}})}{\sigma_{\text{tot}}^0} \equiv \frac{\alpha_s}{2\pi} A(x_{\text{cut}}) + O\left(\alpha_s^2\right). \tag{7}$$

Here, $\alpha_s/(2\pi)\sigma_3^0(x_{\text{cut}})$ denotes the LO cross section for $e^+e^- \to t\bar{t}g$ with $1 - x_{t\bar{t}} > x_{\text{cut}}$ and σ_{tot}^0 is the LO inclusive cross section for $e^+e^- \to t\bar{t}$. The coefficient $A(x_{\text{cut}})$ may be written as follows:

$$A(x_{\text{cut}}) = \frac{2N_C\, C_F \sigma_{\text{pt}}}{\sigma_{\text{tot}}^0} \int_0^1 dx \int_0^1 d\bar{x}\, F_1(x, \bar{x})$$

$$\times \Theta(1 - x_{t\bar{t}} - x_{\text{cut}})\Theta(1 - \cos^2\theta_{t\bar{t}}), \tag{8}$$

where $C_F = (N_C^2 - 1)/(2N_C)$ and $N_C = 3$ is the number of colours. The point cross section σ_{pt} reads

$$\sigma_{\text{pt}} = \sigma(e^+e^- \to \gamma^* \to \mu^+\mu^-) = \frac{4\pi\alpha^2}{3s}, \tag{9}$$

and the LO total cross section σ_{tot}^0 can be expressed in terms of the dimensionless mass variable,

$$z = \frac{m_t^2}{s}, \tag{10}$$

as follows:

$$\sigma_{\text{tot}}^0 = N_C \sigma_{\text{pt}} \sqrt{1 - 4z}\, [c_V(1 + 2z) + c_A(1 - 4z)]. \tag{11}$$

The coupling factors $c_{V,A}$ appearing in (11) are given explicitly by:

$$c_V = Q_t^2\, f^{\gamma\gamma} + 2\, g_V^t\, Q_t\, \text{Re}\chi(s)\, f^{\gamma Z} + g_V^{t\,2}\, |\chi(s)|^2\, f^{ZZ},$$

$$c_A = g_A^{t\,2}|\chi(s)|^2 f^{ZZ}, \tag{12}$$

with

$$f^{\gamma\gamma} = 1 - \lambda_-\lambda_+,$$

$$f^{ZZ} = (1 - \lambda_-\lambda_+)(g_V^{e2} + g_A^{e2}) - 2(\lambda_- - \lambda_+)g_V^e g_A^e,$$

$$f^{\gamma Z} = -(1 - \lambda_-\lambda_+)g_V^e + (\lambda_- - \lambda_+)g_A^e. \tag{13}$$

Here, $Q_t = 2/3$ is the electric charge of the top quark, and $g_{A,V}^f$ denote the axial and vector couplings of the fermion f. In particular, $g_V^e = -\frac{1}{2} + 2\sin^2\vartheta_W$, $g_A^e = -\frac{1}{2}$ for an electron, and $g_V^t = \frac{1}{2} - \frac{4}{3}\sin^2\vartheta_W$, $g_A^t = \frac{1}{2}$ for a top quark, where ϑ_W is the weak mixing angle. The function $\chi(s)$ reads

$$\chi(s) = \frac{1}{4\sin^2\vartheta_W\cos^2\vartheta_W} \frac{s}{s - m_Z^2 + im_Z\Gamma_Z}, \tag{14}$$

where m_Z and Γ_Z stand for the mass and the width of the Z boson. Finally, λ_- (λ_+) denotes the longitudinal polarization of the electron (positron) beam.
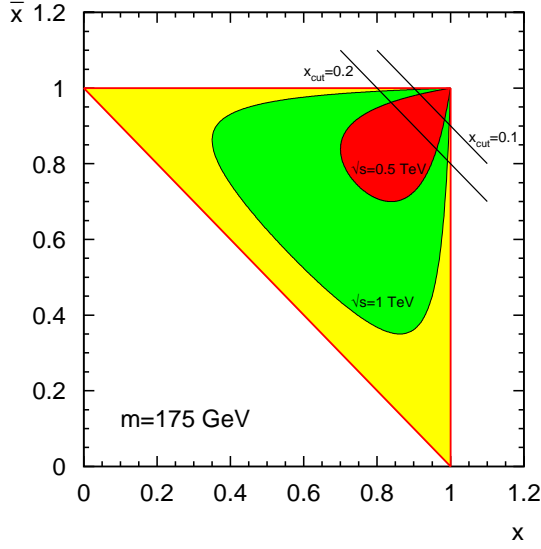
Fig. 1. Kinematically allowed region in the $(x, \bar{x})$ plane for a $t\bar{t}g$ final state with $m_t = 175$ GeV. The enveloping light-coloured triangle is the allowed region for massless quarks. Lines indicate cuts on the scaled gluon energy

The function F_1 may be decomposed as:

$$F_1(x, \bar{x}) = c_V F_1^V(x, \bar{x}) + c_A F_1^A(x, \bar{x}). \qquad (15)$$

Using the abbreviation

$$B = \frac{1}{(1-x)(1-\bar{x})}, \qquad (16)$$

we have [13]:

$$F_1^V(x, \bar{x}) = B \left\{ \frac{x^2 + \bar{x}^2}{2} - z \left[2x_g + \left((1-x)^2 \right. \right. \right.$$
$$\left. \left. \left. + (1-\bar{x})^2 \right) B \right] - 2z^2 x_g^2 B \right\}, \qquad (17)$$

$$F_1^A(x, \bar{x}) = F_1^{VV}(x, \bar{x})$$
$$+ zB \left\{ (x + \bar{x})^2 - 10(1 - x_g) + 6z x_g^2 B \right\}. \ (18)$$

The cosine of the angle between the top quark and antiquark appearing in (8) can be expressed in terms of the top quark mass and the scaled energy variables:

$$\cos \theta_{t\bar{t}} = \frac{x\bar{x} - 2(1 - x_g) + 4z}{\sqrt{(x^2 - 4z)(\bar{x}^2 - 4z)}}. \qquad (19)$$

The Heaviside function $\Theta(1 - \cos^2 \theta_{t\bar{t}})$ defines the kinematically allowed region in the $(x, \bar{x})$ plane when no cuts are applied. For $m_t = 175$ GeV and the two c.m. energies $\sqrt{s} = 0.5$ TeV and $\sqrt{s} = 1$ TeV this region is depicted in Fig. 1. The cuts on the scaled gluon energy $x_{\text{cut}} = 0.1, 0.2$ are indicated as lines, and the enveloping triangle is the kinematically allowed region for massless quarks. With a

cut x_{cut} on the gluon energy, the kinematically allowed area $P(x_{\text{cut}}, z)$ is:

$$P(x_{\text{cut}}, z) \equiv \int_0^1 dx \int_0^1 d\bar{x} \, \Theta(1 - x_{t\bar{t}} - x_{\text{cut}}) \Theta(1 - \cos^2 \theta_{t\bar{t}})$$

$$= \Theta(1 - 4z - x_{\text{cut}}) \left[2z(1 - z) \ln(\rho) \right.$$

$$\left. + \frac{1}{2}(1 - x_{\text{cut}})(1 + x_{\text{cut}} + 2z) \frac{1 - \rho}{1 + \rho} \right], \qquad (20)$$

where

$$\rho = \frac{1 - \sqrt{1 - 4z/(1 - x_{\text{cut}})}}{1 + \sqrt{1 - 4z/(1 - x_{\text{cut}})}}. \qquad (21)$$

When the kinematic boundary $1 - 4z = x_{\text{cut}}$ is approached for a fixed value of x_{cut}, $P(x_{\text{cut}}, z)$ vanishes like $(1 - 4z - x_{\text{cut}})^{3/2}$.

The function $A(x_{\text{cut}})$ defined in (8) can be very easily computed numerically. This has the advantage that an implementation of additional and/or different cuts is straightforward. On the other hand, an analytic result for $A(x_{\text{cut}})$ is obviously desirable, and in fact it is possible to perform the twofold integral in (8) analytically. The result is:

$$A(x_{\text{cut}}) = \frac{2N_C C_F \sigma_{\text{pt}}}{\sigma_{\text{tot}}^0} \Theta(1 - 4z - x_{\text{cut}})$$
$$\times \left[c_V A^V(x_{\text{cut}}) + c_A A^A(x_{\text{cut}}) \right], \qquad (22)$$

where

$$A^V(x_{\text{cut}}) = -\frac{1}{2}(1 + 4x_{\text{cut}} - x_{\text{cut}}^2 + 8z x_{\text{cut}} + 2z^2) \ln(\rho)$$
$$+ \frac{1}{4}(1 - x_{\text{cut}})(11 - 3x_{\text{cut}} + 34z) \frac{1 - \rho}{1 + \rho}$$
$$- (1 - 4z^2) g(\omega, \rho),$$
$$A^A(x_{\text{cut}}) = A^V(x_{\text{cut}}) - z \left[(1 - 4z - 12x_{\text{cut}} - x_{\text{cut}}^2 + 6z^2) \right.$$
$$\times \ln(\rho) + \frac{1}{2}(1 - x_{\text{cut}})(51 + x_{\text{cut}} - 6z) \frac{1 - \rho}{1 + \rho}$$
$$\left. - 6(1 - 2z) g(\omega, \rho) \right], \qquad (23)$$

with

$$g(\omega, \rho) = \ln^2(\omega) - 2\ln\left(\frac{\rho - \omega}{1 - \rho\omega}\right)\left(\ln(\omega) + \frac{1 - \omega^2}{1 + \omega^2}\right)$$
$$+ \ln^2(\rho) + 2\,\text{Li}_2\left(1 - \frac{\rho}{\omega}\right) + 2\,\text{Li}_2\left(1 - \rho\omega\right) \quad (24)$$

and

$$\omega = \frac{1 - \sqrt{1 - 4z}}{1 + \sqrt{1 - 4z}}. \qquad (25)$$

Figure 2 shows the fraction r defined in (6) as a function of the c.m. energy for $m_t = 175$ GeV, and three different values of x_{cut}. Here and in all other numerical results of
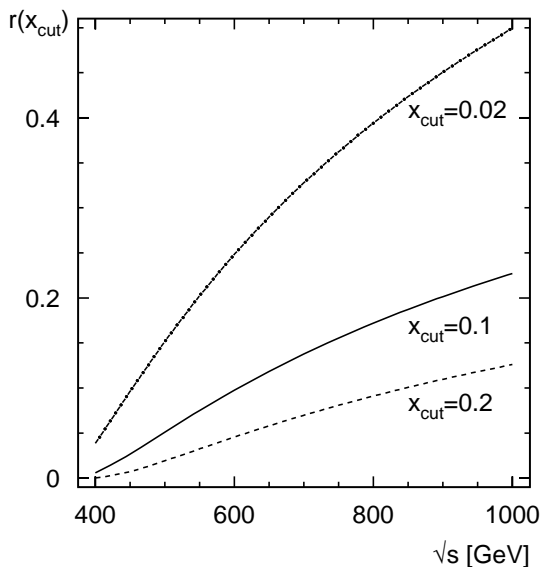
Fig. 2. Fraction $r(x_{\text{cut}})$ (defined in (6)) at leading order in α_s for $x_{\text{cut}} = 0.02, 0.1, 0.2$ and $m_t = 175$ GeV as a function of the center-of-mass energy $\sqrt{s}$. The running of α_s is included

this paper we consider unpolarized electron and positron beams. The running of the strong coupling is taken into account in the curves, i.e. we use $\alpha_s(\mu = \sqrt{s})$ with six active flavours. Our input value is $\alpha_s^{n_f=5}(\mu = m_Z) = 0.118$, which is evolved up to $\mu = m_t$ with five active flavours, and then converted into $\alpha_s^{n_f=6}(m_t)$ using the so-called matching conditions of [14][1]. For example, we thus get $\alpha_s^{n_f=6}(\mu = 500 \text{ GeV}) = 0.0952$.

We close this section with a remark concerning the experimental distinction of $t\bar{t}$ events with a gluon radiated off the t or $\bar{t}$ from events in which the gluon is radiated off the b or $\bar{b}$ produced in the decays of the top quark pairs. It has been shown in [15] that the following two constraints efficiently select events where the gluon is produced in association with the top quark pair:

$$E_g > \frac{\sqrt{s}}{2} x_{\text{cut}} \gg \Gamma_t,$$

$$m_t - 2\Gamma_t \leq \sqrt{\left(k_{W^\pm} + k_{b(\bar{b})}\right)^2} \leq m_t + 2\Gamma_t. \quad (26)$$

By requiring that the invariant mass of the Wb system lies in the vicinity of the top quark mass, the probability that a highly energetic gluon jet ($E_g \gg \Gamma_t \approx 1.4$ GeV) is emitted from the b or $\bar{b}$ is very small. Our computation may therefore be applied to describe events of the type $e^+ e^- \to W^+ W^- b\bar{b}g$ that fulfil both conditions of (26). Our "default" value for many of the results below will be $x_{\text{cut}} = 0.1$, which corresponds to $E_g = 25$ (50) GeV for a c.m. energy $\sqrt{s} = 0.5$ (1) TeV.

3 Results at next-to-leading order

At order α_s^2, we have to consider both virtual and real corrections to the process (2). The real corrections consist of the processes $e^+ e^- \to t\bar{t}gg$, $e^+ e^- \to t\bar{t}q\bar{q}$ ($q = u, d, s, c, b$). If $\sqrt{s} > 4m_t$, the production of *two* $t\bar{t}$ pairs becomes possible. However, these rather spectacular events are extremely rare for the c.m. energies considered below and contributions from the process $e^+ e^- \to t\bar{t}t\bar{t}$ can therefore be neglected[2].

As mentioned before, the condition $1 - x_{t\bar{t}} > x_{\text{cut}}$ is equivalent, at LO, to requiring a minimal scaled gluon energy x_g. For final states with four or more partons, an alternative condition is $2kk_X/s > x_{\text{cut}}$, where in the c.m. system $2kk_X/s$ is equal to $2E_X/\sqrt{s}$, with $E_X = \sqrt{s} - E_t - E_{\bar{t}}$. For a given cut x_{cut}, this condition leads to larger contributions to $r(x_{\text{cut}})$ from the four-parton final states as compared to the definition employed in (6), since $2E_X/\sqrt{s} = 1 - x_{t\bar{t}} + k_X^2/s$ with $k_X^2 \geq 0$.

We renormalize the coupling in the modified minimal subtraction ($\overline{\text{MS}}$) scheme. For the results of this section, the top quark mass is defined as the perturbative pole mass, i.e., the mass renormalization is carried out in the on-shell scheme. The result for the fraction $r(x_{\text{cut}})$ at a renormalization scale μ may be written to next-to-leading accuracy as

$$r(x_{\text{cut}}, \mu) = \frac{\sigma_3(x_{\text{cut}}, \mu)}{\sigma_{\text{tot}}(\mu)}$$
$$= \frac{\alpha_s(\mu)}{2\pi} A(x_{\text{cut}}) + \left(\frac{\alpha_s(\mu)}{2\pi}\right)^2 B(x_{\text{cut}}, \mu)$$
$$+ O\left(\alpha_s^3\right), \quad (27)$$

with

$$\sigma_3(x_{\text{cut}}, \mu) = \frac{\alpha_s(\mu)}{2\pi} \sigma_3^0(x_{\text{cut}}) + \left(\frac{\alpha_s(\mu)}{2\pi}\right)^2 \sigma_3^1(x_{\text{cut}}, \mu)$$
$$+ O\left(\alpha_s^3\right), \quad (28)$$

$$\sigma_{\text{tot}}(\mu) = \sigma_{\text{tot}}^0 + \frac{\alpha_s(\mu)}{2\pi} \sigma_{\text{tot}}^1 + O\left(\alpha_s^2\right). \quad (29)$$

The coefficient $A(x_{\text{cut}})$ is given explicitly in (22), (23), and the coefficient $B(x_{\text{cut}}, \mu)$ reads:

$$B(x_{\text{cut}}, \mu) = \frac{\sigma_3^1(x_{\text{cut}}, \mu)}{\sigma_{\text{tot}}^0} - \frac{\sigma_{\text{tot}}^1 \sigma_3^0(x_{\text{cut}})}{\left(\sigma_{\text{tot}}^0\right)^2}. \quad (30)$$

The result for σ_{tot}^1 is well known (see, e.g. [16]). For the computation of $\sigma_3^1(x_{\text{cut}}, \mu)$ we use the techniques and results of [17] and [13]. In these papers, the production of three jets involving b quarks was studied at NLO, taking into account the b quark mass. The matrix elements given there can be easily adapted to the case at hand. For technical details of the calculation, we refer the reader to [13].

---

[1] To be more precise, the conversion is performed at the scale $\overline{m}_t(\overline{m}_t)$, where $\overline{m}_t$ is the running top quark mass

[2] Contributions from "secondary" t-quarks, originating from gluon splitting in $e^+ e^- \to q\bar{q}g$, are also heavily suppressed
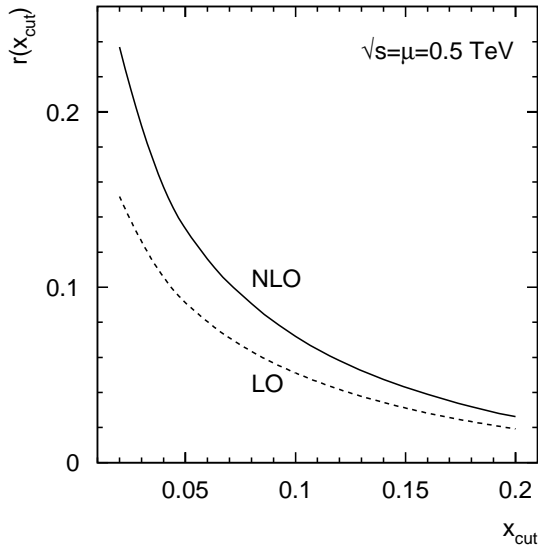
Fig. 3. Fraction $r(x_{\mathrm{cut}})$ at leading (LO) and next-to-leading order (NLO) as a function of x_{cut} at $\sqrt{s} = 0.5$ TeV. The renormalization scale μ is set to $\sqrt{s}$
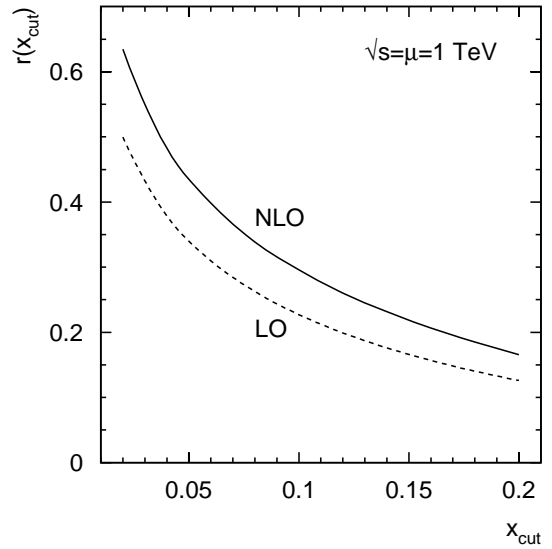
Table 1. Leading order and next-to-leading order coefficients of the fraction $r(x_{\mathrm{cut}}, \mu)$ as defined in (27) for two different center-of-mass energies and $x_{\mathrm{cut}} = 0.1$. The renormalization scale μ is set to $\sqrt{s}$, and a top quark pole mass of $m_t = 175$ GeV is used

x_{cut}	$\sqrt{s} = 0.5$ TeV		$\sqrt{s} = 1$ TeV	
	A	B	A	B
0.02	10.02	371(2)	35.46	680(3)
0.04	6.976	224(2)	26.87	524(3)
0.06	5.302	156(2)	21.99	447(3)
0.08	4.185	119(2)	18.64	384(3)
0.10	3.373	90.6(12)	16.12	347(3)
0.12	2.751	71.5(10)	14.13	309(3)
0.14	2.260	57.1(10)	12.50	280(3)
0.16	1.864	46.9(10)	11.12	251(2)
0.18	1.539	36.9(10)	9.957	226(2)
0.20	1.271	30.1(8)	8.945	200(2)

Figure 3 (4) shows the LO and NLO results for r as a function of x_{cut} at $\sqrt{s} = 0.5$ TeV ($\sqrt{s} = 1$ TeV). The renormalization scale is set to $\mu = \sqrt{s}$. (The scale dependence of our results will be discussed in the next section.) In Table 1 we list the A and B coefficients for a sample of x_{cut}-values. The numerical errors in the last digits of the B coefficients are also shown[3]. For $\sqrt{s} = 0.5$ TeV, the relative size of the QCD corrections, $\alpha_s/(2\pi)B/A$, varies between 56% (at $x_{\mathrm{cut}} = 0.02$) and 36% (at $x_{\mathrm{cut}} = 0.2$). At $\sqrt{s} = 1$ TeV, the QCD corrections are roughly constant as x_{cut} is varied and of the order of 30%. In Figs. 5, 6, and 7 we plot various distributions of the cross section $\sigma_3(x_{\mathrm{cut}}, \mu)$. All distributions are normalized to the total $t\bar{t}$
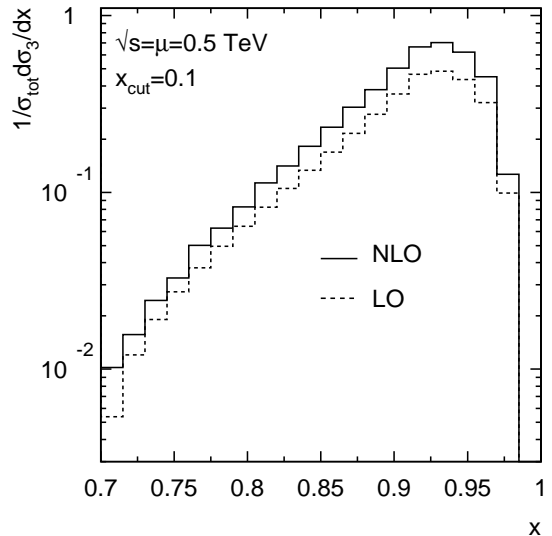
---

[3] For example, 57.1(10) stands for 57.1 ± 1.0

Fig. 4. Same as Fig. 3, but for $\sqrt{s} = 1$ TeV

Fig. 5. Distribution $1/\sigma_{\mathrm{tot}}d\sigma_3/dx$ at LO and NLO for $\sqrt{s} = \mu = 0.5$ TeV and $x_{\mathrm{cut}} = 0.1$. The scaled quark energy is defined in (3), and the cross section σ_3 is defined in (27)

cross section σ_{tot}, and we set $\sqrt{s} = \mu = 0.5$ TeV, $m_t = 175$ GeV, and $x_{\mathrm{cut}} = 0.1$. These values lead to the kinematic limits $0.7 \leq x \lesssim 0.9837$, $0.1 \leq 1 - x_{t\bar{t}} \leq 0.51$ for the scaled top quark energy x and the quantity $1 - x_{t\bar{t}}$, respectively. (Recall that in leading order $1 - x_{t\bar{t}}$ is equal to the scaled gluon energy x_g.) Figure 5 shows the distribution $1/\sigma_{\mathrm{tot}}d\sigma_3/dx$. The distribution reaches its maximum around $x \approx 0.925$, which corresponds to $E_t \approx 231$ GeV. We note in passing that the distribution with respect to the scaled top antiquark energy $\bar{x}$ is equal to the one shown due to charge conjugation invariance of the strong interactions. In Fig. 6 we plot the distribution $1/\sigma_{\mathrm{tot}}d\sigma_3/d(1 - x_{t\bar{t}})$. The size of the QCD corrections depends only weakly on $1 - x_{t\bar{t}}$. Figure 7 depicts the distribution with respect to the cosine of the angle between the
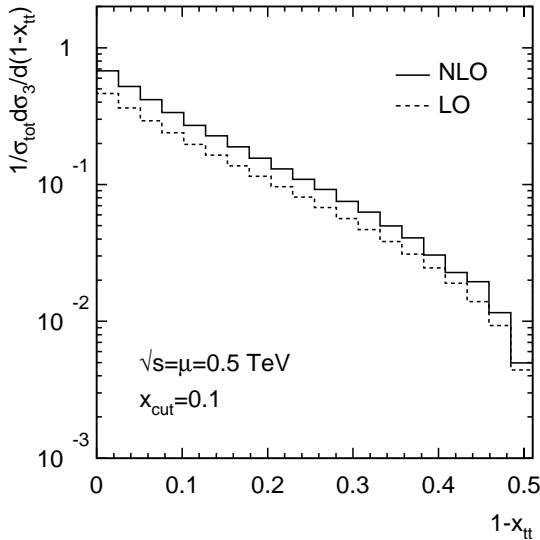
Fig. 6. Same as Fig. 5, but for $1/\sigma_{\text{tot}}d\sigma_3/d(1-x_{t\bar{t}})$ with $x_{t\bar{t}}$ defined in (3)
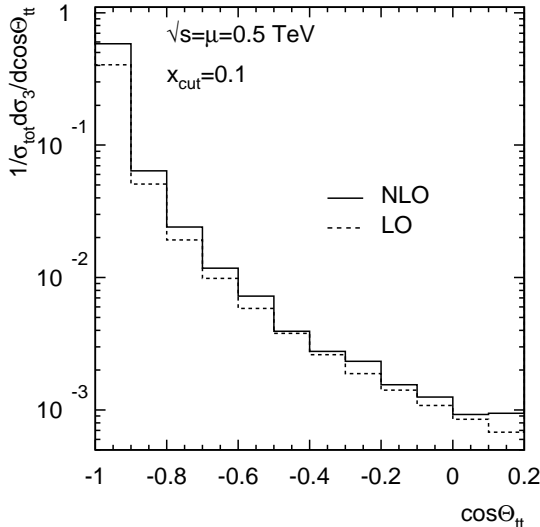

Fig. 7. Same as Fig. 5, but for $1/\sigma_{\text{tot}}d\sigma_3/d(\cos\theta_{t\bar{t}})$ with $\cos\theta_{t\bar{t}}$ defined in (19)

top quark and antiquark. As one might have expected, this distribution is very sharply peaked close to $\cos\theta_{t\bar{t}} = -1$.

4 Top quark pole mass versus running mass

All results in the preceding section have been obtained by using the $\overline{\text{MS}}$ scheme for the coupling renormalization and by renormalizing the top quark mass in the on-shell scheme. In this section we study the dependence of our results on the mass renormalization scheme as well as on the choice of the renormalization scale μ.

In order to understand the impact of a change of the mass definitions on our fixed order predictions, it is instructive first to consider the simple and well-known case of the inclusive rate σ_{tot}. We use the notation $z^{\text{on}} = (m_t^{\text{on}})^2/s$ and $\overline{z}(\mu) = \overline{m}_t^2(\mu)/s$, where m_t^{on} is the pole

mass (for which we always use the value $m_t^{\text{on}} = 175$ GeV) and $\overline{m}_t(\mu)$ is the $\overline{\text{MS}}$ mass at a scale μ. The latter is obtained from the renormalization group evolution with the input $\overline{m}_t(\mu = \overline{m}_t) = 168$ GeV. The relation between the two mass parameters is given by

$$z^{\text{on}} = \overline{z}(\mu) + \Delta\overline{z}(\mu), \tag{31}$$

where, to order α_s,

$$\Delta\overline{z}(\mu) = \frac{2C_F\alpha_s(\mu)}{\pi}\left[1 - \frac{3}{4}\ln\left(\frac{\overline{z}(\mu)s}{\mu^2}\right)\right]\overline{z}(\mu)$$
$$+ O\left(\alpha_s^2\right). \tag{32}$$

To order α_s we thus have[4]:

$$\sigma_{\text{tot}}(z^{\text{on}}, \mu) = \sigma_{\text{tot}}(\overline{z}(\mu) + \Delta\overline{z}(\mu), \mu)$$
$$= \sigma_{\text{tot}}^0(\overline{z}(\mu)) + \Delta\overline{z}(\mu)\frac{d\sigma_{\text{tot}}^0}{dz}(\overline{z}(\mu))$$
$$+ \frac{\alpha_s(\mu)}{2\pi}\sigma_{\text{tot}}^1(\overline{z}(\mu)) + O\left(\alpha_s^2\right), \tag{33}$$

where $d\sigma_{\text{tot}}^0/dz$ can be obtained from (11). Figure 8 (9) shows the total cross section in units of the point cross section (9) as a function of the renormalization scale at $\sqrt{s} = 0.5$ TeV ($\sqrt{s} = 1$ TeV) for both mass definitions. When σ_{tot} is expressed in terms of the pole mass, the dependence on μ is (to order α_s) only induced by the running of α_s. Two important features are visible in the curves: First, within a large range of values for μ, the QCD corrections are smaller when the result is expressed in terms of the running mass. Second, the μ dependence is flatter if the running mass is used. For small values of μ one further observes a strong decrease (increase) of the LO (NLO) prediction for σ_{tot} expressed in terms of the running mass. These unphysical features occur because *both* the coupling *and* the running mass become large as μ becomes small[5]. The decrease of the LO result simply reflects the fact that σ_{tot}^0 goes to zero as z approaches the threshold value $z = 1/4$. The fact that the NLO result in both mass renormalization schemes is rather stable when μ is varied as well as the good agreement of the predictions in the two schemes indicates that the contributions of order α_s^2 are small. As the explicit calculation of [4] shows, this is indeed the case for energies well above the top quark production threshold.

We now turn back to the discussion of the fraction $r(x_{\text{cut}})$. The renormalization scale dependence of the NLO coefficient B in the pole mass scheme is easily obtained:

$$B(x_{\text{cut}}, z^{\text{on}}, \mu) = B(x_{\text{cut}}, z^{\text{on}}, \sqrt{s})$$
$$- A(x_{\text{cut}}, z^{\text{on}})\beta_0\ln\left(\frac{\sqrt{s}}{\mu}\right), \tag{34}$$

with $\beta_0 = (11N_C - 2n_f)/3$ and $n_f = 6$. In analogy to (33) we may express the result for $r(x_{\text{cut}})$ in terms of the $\overline{\text{MS}}$ mass at the scale μ by writing

---

[4] I thank M. Spira for explaining to me this method of switching between two mass renormalization schemes

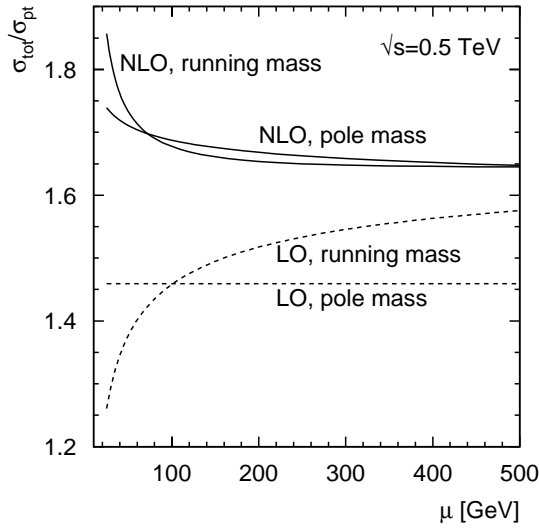[5] For example, at $\mu = 25$ GeV we have $\overline{m}_t(\mu = 25 \text{ GeV}) \approx 199.3$ GeV

Fig. 8. LO and NLO results for the total $t\bar{t}$ cross section in units of the point cross section defined in (9) at a c.m. energy of $\sqrt{s} = 0.5$ TeV. The renormalization scale μ is varied between 25 GeV and $\sqrt{s}$, and results obtained in the pole mass and in the $\overline{\text{MS}}$ (running) mass renormalization schemes are compared
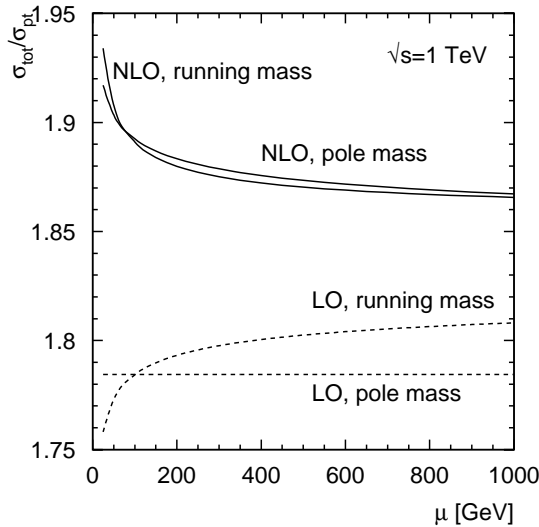

Fig. 9. Same as Fig. 8, but for $\sqrt{s} = 1$ TeV

$$r(x_{\text{cut}}, z^{\text{on}}, \mu) = r(x_{\text{cut}}, \overline{z}(\mu) + \Delta\overline{z}(\mu), \mu)$$
$$= \frac{\alpha_s(\mu)}{2\pi} A\left(\overline{z}(\mu)\right) + \Delta\overline{z}(\mu)\frac{dA}{dz}\left(\overline{z}(\mu)\right)$$
$$+ \left(\frac{\alpha_s(\mu)}{2\pi}\right)^2 B(x_{\text{cut}}, \overline{z}(\mu), \mu) + O\left(\alpha_s^3\right). \quad (35)$$

Figures 10 and 11 show the LO and NLO results for r at $x_{\text{cut}} = 0.1$ as a function of μ both in the pole mass and the running mass scheme at $\sqrt{s} = 0.5$ TeV and $\sqrt{s} = 1$ TeV, respectively. At $\sqrt{s} = 0.5$ TeV, we find a rather large difference of the NLO results in the two schemes at scales $\mu \sim \sqrt{s}$. The additional gluon in the final state carries (at $x_{\text{cut}} = 0.1$) a momentum of at least 25 GeV, and the allowed phase space depends rather strongly on the
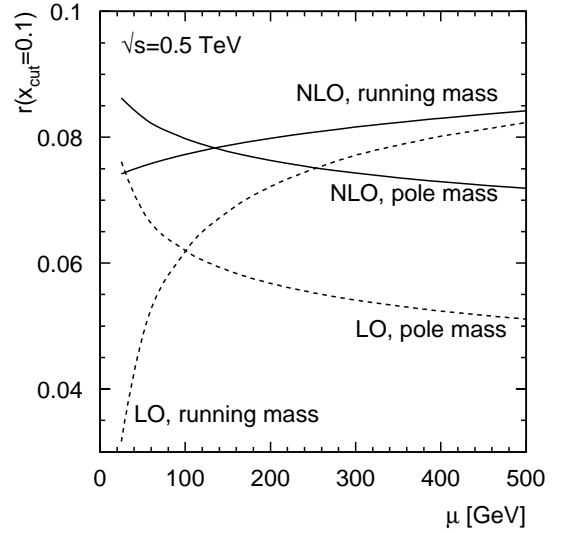

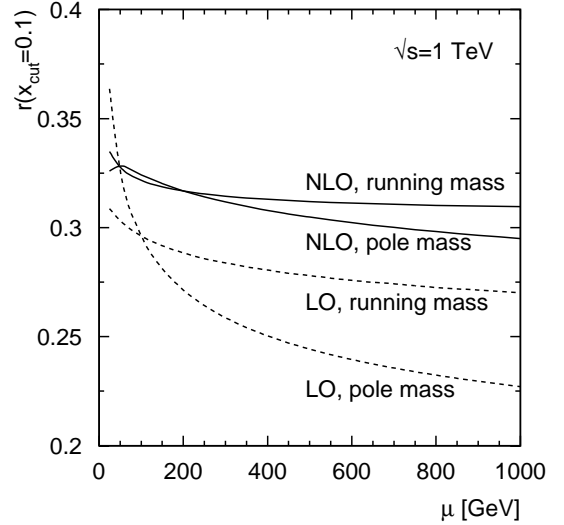**Fig. 10.** Same as Fig. 8, but for the fraction r at $x_{\text{cut}} = 0.1$

Fig. 11. Same as Fig. 10, but for $\sqrt{s} = 1$ TeV

top quark mass[6], which explains the strong μ-dependence of the LO result in terms of the running mass. At NLO the μ-dependence is drastically reduced, but r still increases with μ. The gain in phase space due to the decrease of $\overline{m}_t(\mu)$ overcompensates the decrease of $\alpha_s(\mu)$ even at NLO. This suggests that the running mass should not be used in the fixed-order prediction for the fraction r at $\sqrt{s} = 0.5$ TeV and $x_{\text{cut}} \geq 0.1$. At these values, we are too close to the kinematic threshold of the $t\bar{t}g$ final state where the running mass is an "unnatural" parameter.

At $\sqrt{s} = 1$ TeV the differences of the NLO results for the two mass definitions are smaller as compared to the case of $\sqrt{s} = 0.5$ TeV. Also, the NLO results only weakly depend on the choice of μ, especially if the running mass is used. The two scales m_t and $\sqrt{s}$ are now rather far apart, and the running mass parameter becomes preferable. For

---

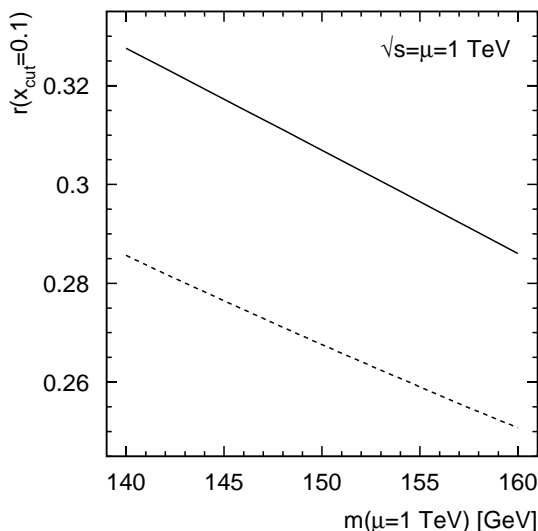[6] The running top quark mass decreases from 199.3 GeV to 155.3 GeV as μ is varied between 25 and 500 GeV

Fig. 12. Dependence of the fraction r at $x_{\text{cut}} = 0.1$ and $\sqrt{s} = \mu = 1$ TeV on the value of the running top quark mass $\overline{m}_t$ at the scale $\mu = 1$ TeV. The dashed line is the LO result, and the solid line is the NLO result

even higher c.m. energies, the fraction r as defined in (6) eventually suffers from large contributions in the collinear region; as $z \to 0$, the result in nth order is dominated by terms $\sim (\alpha_s \ln(z))^n$, which should either be resummed or avoided by modifying the definition of r. One could for example, after selecting samples of $t\bar{t}X$ events with $1 - x_{t\bar{t}} > x_{\text{cut}}$, use in addition standard jet algorithms to define collinear safe cross sections.

An intriguing question is whether a measurement of the fraction r allows a direct determination of the value of the running mass parameter of the top quark at high energies. (Analogously, NLO results for three-jet fractions involving b quarks [18,17,13] have been used to extract a value for $\overline{m}_b(\mu = m_Z)$ from the high-statistics LEP [19] and SLD [20,21] data.) We consider here as a case study the result for $r(x_{\text{cut}} = 0.1)$ at $\sqrt{s} = 1$ TeV. As was discussed above, for these values the fraction r is perturbatively well under control when expressed in terms of the running mass. We now vary the value $\overline{m}_t(\mu = 1$ TeV) between 140 and 160 GeV[7] and compute $r(x_{\text{cut}} = 0.1)$ at LO and NLO. The results are shown in Fig. 12. At NLO, $r(x_{\text{cut}} = 0.1)$ decreases by about 4% when the running top quark mass is changed from 140 to 160 GeV. If a measurement of r will be possible with an error of $\pm 1\%$, the running top quark mass at $\mu = 1$ TeV could be determined up to ± 5 GeV. A statistical error of 1% on r is realistic with the envisioned high luminosity of a future linear collider operating at $\sqrt{s} = 1$ TeV, but whether or not the systematic error can be kept that small remains to be seen.

Although the sensitivity of the fraction r on $\overline{m}_t(\mu = 1$ TeV) seems to be rather poor, a direct determination of the running top quark mass at such a high scale would

provide a nice test of perturbative QCD in the following way: It is expected that a very precise value of the top quark mass can be obtained from the threshold scan of σ_{tot}. Since the pole mass suffers from (nonperturbative) infrared ambiguities, improved mass definitions have been proposed in this context, the so-called potential-subtracted [5,6] and 1S [7] mass. After extracting these masses from the threshold scan, they can be converted into the $\overline{\text{MS}}$ mass, evolved to $\mu = 1$ TeV, and compared to the direct measurement suggested above.

5 Conclusions

At a future high-energy and high-luminosity e^+e^- linear collider, the production of top quark pairs in association with one or more additional hard partons will be an interesting new testing ground for perturbative QCD. For example, a measurement of the fraction r of $t\bar{t}X$ events with respect to all $t\bar{t}$ events will provide a powerful "flavour independence test" of the strong interactions. In this paper we have studied the reaction $e^+e^- \to t\bar{t}X$ to order α_s^2. The fraction r has been defined as a function of a preset cut parameter x_{cut} by demanding $1 - x_{t\bar{t}} > x_{\text{cut}}$ where $x_{t\bar{t}} = (k_t + k_{\bar{t}})^2/s$ is the scaled invariant mass square of the $t\bar{t}$ pair. At LO, where $1 - x_{t\bar{t}}$ is equal to the scaled gluon energy $x_g = 2E_g/\sqrt{s}$, we have calculated this fraction analytically. The QCD corrections to $r(x_{\text{cut}})$, which we have evaluated for c.m. energies $\sqrt{s} = 0.5$ TeV and $\sqrt{s} = 1$ TeV, are large and positive. We have further computed distributions of the differential cross section for $e^+e^- \to t\bar{t}X$ with respect to the scaled top quark energy, the variable $1 - x_{t\bar{t}}$, and the cosine of the angle between t and $\bar{t}$. A measurement of such distributions will be interesting for instance in the context of searches for possible anomalous top quark couplings, and the QCD corrections have to be included in such analyses. Finally we have studied the dependence of our results on the renormalization scale μ and compared the pole mass and the running mass renormalization schemes. We have found that at $\sqrt{s} = 0.5$ TeV the phase space for $t\bar{t}g$ production depends (for a hard gluon) rather strongly on the value of the top quark mass parameter. We have concluded that for this (or smaller) c.m. energies the fixed order prediction for the fraction r should not be expressed in terms of the running mass. At $\sqrt{s} = 1$ TeV, $\overline{m}_t(\mu)$ becomes the preferable mass parameter. This is reflected in the improved stability of the NLO results under variations of the scale μ. If a measurement of r at $\sqrt{s} = 1$ TeV is possible to an accuracy of 1%, the running mass $\overline{m}_t(\mu = 1$ TeV) could be directly determined up to about ± 5 GeV, offering a nice consistency check of the renormalization group evolution of $\overline{m}_t(\mu)$ as predicted by perturbative QCD.

In this paper we have concentrated on studying the fraction of $t\bar{t}X$ events and their distributions with respect to energies of and angles between final state particles only. Future work will include the investigation of observables that involve the orientation of the final state with respect to the electron beam, like forward-backward asymmetries or so-called "event handedness" correlations [10].

---

[7] The value obtained from the renormalization group evolution is $\overline{m}_t(\mu = 1$ TeV$) = 148.6$ GeV

References

1. A.H. Hoang and T. Teubner, Phys. Rev. **D 58** (1998) 114023.
2. K. Melnikov and A. Yelkhovsky, Nucl. Phys. **B 528** (1998) 59; O. Yakovlev, hep-ph/9808463.
3. J.H. Kühn and T. Teubner, TTP-99-12, hep-ph/9903322 (1999).
4. K.G. Chetyrkin *et al.*, Eur. Phys. J. **C 2** (1998) 137.
5. M. Beneke, A. Signer, and V.A. Smirnov, CERN-TH-99-57, hep-ph/9903260 (1999).
6. T. Nagano, A. Ota, Y. Sumino, TU-562, hep-ph/9903498 (1999).
7. A.H. Hoang and T. Teubner, CERN-TH/99-59, DESY 99-047, hep-ph/9904468 (1999).
8. T.G. Rizzo, Phys. Rev. **D 50** (1994) 4478; SLAC-PUB-7317, hep-ph/9610373 (1996).
9. S. Bar-Shalom, D. Atwood, G. Eilam, and A. Soni, Z. Phys. **C 72** (1996) 79.
10. A. Brandenburg, L. Dixon, and Y. Shadmi, Phys. Rev. **D 53** (1996) 1264.
11. K. Abe *et al.* (SLD Collab.), SLAC-PUB-7920, hep-ex/9903004 (1999).
12. K. Abe *et al.* (SLD Collab.), Phys. Rev. Lett. **75** (1995) 4173; SLAC-PUB-7823 (1998).
13. A. Brandenburg and P. Uwer, Nucl. Phys. **B 515** (1998) 279.
14. W. Bernreuther and W. Wetzel, Nucl. Phys. **B 197** (1982) 228; Erratum-ibid. **B 513** (1998) 758; K.G. Chetyrkin, B.A. Kniehl, M. Steinhauser, Nucl. Phys. **B 510** (1998) 61.
15. C. Macesanu, L.H. Orr, UR-1542, ER/40685/921, hep-ph/9808403 (1998).
16. K.G. Chetyrkin, J.H. Kühn, and A. Kwiatkowski, Phys. Rep. **277** (1996) 189.
17. W. Bernreuther, A. Brandenburg, and P. Uwer, Phys. Rev. Lett. **79** (1997) 189.
18. G. Rodrigo, A. Santamaria, and M. Bilenky, Phys. Rev. Lett. **79** (1997) 193.
19. P. Abreu *et al.* (DELPHI Collab.), Phys. Lett. **B 418** (1998) 430.
20. P.N. Burrows, SLAC-PUB-7914 (1998); to appear in Proc. XXIX International Conf. on High Energy Physics, Vancouver, Canada, July 23-29 1998.
21. A. Brandenburg, P.N. Burrows, D. Muller, N. Oishi, and P. Uwer, SLAC-PUB-7915, OUNP-99-06, Saclay/SPhT-T99/047, PITHA 99/12, hep-ph/9905495 (1999).